

Soft-contact imaging in liquid with frequency-modulation torsion resonance mode atomic force microscopy

This article has been downloaded from IOPscience. Please scroll down to see the full text article.

2010 Nanotechnology 21 065710

(<http://iopscience.iop.org/0957-4484/21/6/065710>)

View [the table of contents for this issue](#), or go to the [journal homepage](#) for more

Download details:

IP Address: 140.109.103.227

The article was downloaded on 25/05/2011 at 05:26

Please note that [terms and conditions apply](#).

Soft-contact imaging in liquid with frequency-modulation torsion resonance mode atomic force microscopy

Chih-Wen Yang and Ing-Shouh Hwang¹

Institute of Physics, Academia Sinica, Nankang, Taipei 115, Taiwan, Republic of China

E-mail: ishwang@phys.sinica.edu.tw

Received 2 October 2009, in final form 8 December 2009

Published 8 January 2010

Online at stacks.iop.org/Nano/21/065710

Abstract

In this work, we demonstrate that high-resolution imaging in water with a soft contact between the tip and the sample can be achieved with frequency-modulation torsional resonance (FM-TR) mode atomic force microscopy (AFM). This mode is very sensitive to the contact of the tip with the sample surface. A sharp jump in the resonance frequency shift occurs when the tip is getting in touch with the sample. Individual atomic features on mica surfaces can be resolved with a relatively large tip. The tip applies very small normal and lateral forces on the surface. In addition, even a long and compliant AFM cantilever can achieve a high quality factor and a high resonant frequency for the torsional oscillation in water. Along with several other advantages, this mode is very suitable for future development of high-sensitivity, high-resolution, high-speed AFM for the study of dynamic biological processes in liquid.

(Some figures in this article are in colour only in the electronic version)

1. Introduction

To unravel many puzzles in life sciences, high-resolution imaging of biological samples in aqueous or physiological conditions is essential. Optical microscopy is a major technique in imaging biological molecules, but diffraction limits its resolution to about half the wavelength. Atomic force microscopy (AFM) [1, 2] and its related scanning probe microscopies are among the few techniques that can achieve resolution down to the nanometer or sub-nanometer scale in liquid. Contact mode AFM is often used to image in liquid; however, the large normal and lateral forces of the AFM tip tends to deform, damage or dislodge soft materials during scanning. It has been recommended that the loading force for the tip apex on biomolecules should be lower than 100 pN in order to obtain the undistorted structure of the soft molecules [3].

The tapping mode is generally believed to apply a more gentle force than the contact mode. In this mode, the tip is oscillated vertically (perpendicular to the sample surface) at or near the resonant frequency of the AFM cantilever

and the reduction of the vibrational amplitude is used as the feedback signal for adjusting the tip-sample spacing. However, the force sensitivity is significantly reduced in liquid due to the low quality factor ($Q < 10$) for the resonance of typical cantilevers. An alternative approach is the adoption of the frequency-modulation (FM) detection scheme [4, 5], in which the feedback system keeps a constant resonant frequency shift during image acquisition. It has been demonstrated that FM-AFM can resolve individual atoms on several hard, flat surfaces in vacuum [5–12]. It has also been shown that the FM detection scheme provides a better force sensitivity than the tapping mode, or the amplitude modulation (AM) detection scheme, with the same tip under the same environment [13]. In recent years, atomic resolution on mica surfaces in liquid was also achieved with the FM mode by a few groups [14–16]. However, they used relatively stiff AFM cantilevers (spring constant $k > 20 \text{ N m}^{-1}$), which are not suitable for certain experiments. For example, it is often desirable to use compliant AFM cantilevers to carry out force-displacement measurements such as single-molecule force spectroscopy [17, 18].

All of the above AFM modes use the flexural bending (static or dynamic) of the cantilever as the feedback input to

¹ Author to whom any correspondence should be addressed.

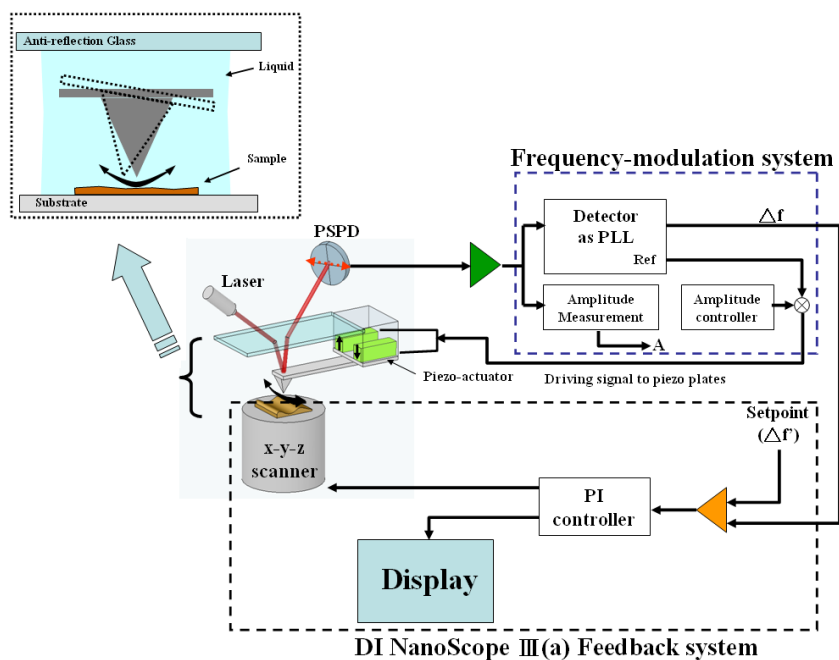


Figure 1. Schematic of our set-up for FM-TR mode AFM. Inset: a drop of liquid is introduced between the substrate and the anti-reflection glass. The torsion vibration of the tip is also illustrated.

maintain the tip-sample separation. The torsion resonance (TR) mode is very different from the above flexural modes. In this mode, the cantilever executes small torsion resonant oscillations by twisting about its long axis, and the cantilever's free end rotates a very small angle about that axis. The AFM tip apex then executes very small pendulum-like oscillations in the lateral direction (parallel to the sample surface). This mode was initially developed to map in-plane mechanical properties on hard surfaces, such as friction, shear stiffness and other tribologically relevant properties [19–22], and is typically operated in air with the TR amplitude as the feedback input.

In this work, our feedback system tracks the resonant frequency shift of the torsion-vibrating cantilever to maintain a soft contact during AFM imaging. Even long and compliant cantilevers can achieve good torsion resonance with a high quality factor in water. Most importantly, a sharp jump in the resonant frequency shift occurs when the tip is getting in touch with the sample, which allows clear detection of the contact point and maintaining a soft contact between the tip apex and the surface. When probing a soft material with the flexural modes, it is relatively difficult to determine the contact point because most long-range forces, such as electrostatic and van der Waals forces, are acting in the normal direction. Thus it is not easy to distinguish whether the change in the force (or the force gradient) is caused by contact with soft matter or by the long-range interactions. In contrast, the TR mode is only affected by the lateral force gradient acting on the tip. If no long-range lateral forces are present, which is usually the case, the lateral forces start to occur only when the tip is getting in contact with the sample surface.

2. Experimental details

Our experiments are carried out using a system based on a commercial beam-deflection AFM (DI NanoScope III(a) from Digital Instrument, Santa Barbara, CA). Figure 1 shows a schematic of our set-up for FM-TR mode AFM. The tip holder has been modified for the torsion excitation and operation in water. The torsional oscillation of the cantilever is excited by driving two dither piezo-elements with two sinusoidal signals of the same frequency but 180° out of phase. This excitation method was also described previously [22]. The FM modes are implemented with an easyPLL unit (Nanosurf® easyPLL plus system) through a Signal Access Module (Digital Instrument, Santa Barbara, CA) [13]. The easyPLL unit is applied to track the resonant frequency of the vibrating cantilever. During scanning, the frequency shift of torsion resonance of the cantilever is used as the feedback signal of a PI controller, which outputs a z signal to drive a piezo-scanner tube. The sample displacement is driven by the piezo-scanner under the sample stage. In our AFM imaging and measurements of the resonance frequency shift versus sample displacement curves, we use the constant-excitation mode, in which an oscillation signal with a constant amplitude is applied to the piezo-elements to drive the motion of the cantilever. The AFM images are two-dimensional maps of the sample displacement (or z piezo-displacement, Δz). They are not the same as the topographic images when compliant cantilevers are used, as will be explained later.

The mica substrates used here are not pure muscovite mica. They are obtained from electronics shops and are typically used as insulators for electronic devices. The mica substrates are cleaved right before the AFM experiments or DNA adsorption. The duplex DNA was isolated from

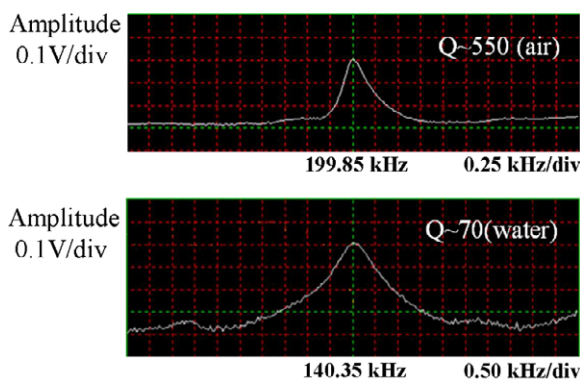


Figure 2. Typical torsional vibration amplitude of the cantilever as a function of the excitation frequency in air and in water.

bacteriophage lambda (cl857ind 1 Sam 7). Since DNA and the mica surface are negatively charged in pure water, we use Ni^{2+} ions to immobilize DNA on the surface. $20 \mu\text{l}$ of a mixed solution of DNA ($5 \text{ ng } \mu\text{l}^{-1}$) and Ni^{2+} (3 mM) is dropped onto a freshly cleaved mica surface. After waiting for ~ 3 min, the buffer solution is removed with filter paper. This sample is then placed onto the AFM stage and pure water (5 ml) is introduced between the sample and the anti-reflection glass plate [16]. As shown in the inset at the upper-left side of figure 1, the torsion vibration of the cantilever in liquid is illustrated. The anti-reflection glass plate helps the trapping of the water droplet and also provides a stable interface for the detection laser beam. We usually wait for about 1 h before the acquisition of AFM images is started, because thermal drift becomes less serious after that point.

The lateral force and the torsional deflection can be calculated from the friction loop measurement [23] and the estimated torsional spring constant. In the sticking part of the friction loop, the tip sticks to the substrate. From the scan movement driven by the piezo-scanner and the detected lateral displacement signal (X signal) from the quadrant photosensor, their relation can be determined. The corresponding torsional deflection angle can also be estimated from the tip height and

the scan movement. The torsional spring constant is estimated with the method proposed by Jeon and Braiman [24].

3. Results and discussion

3.1. Torsional oscillation in water

In our FM-TR AFM operation, we use a type of compliant silicon cantilever with Au-coated tips (MikroMasch, CSC38/Cr-Au, $350 \mu\text{m} \times 35 \mu\text{m} \times 1 \mu\text{m}$, $k = 0.01\text{--}0.08 \text{ N m}^{-1}$, nominal tip radius $\sim 50 \text{ nm}$) because these cantilevers can achieve nearly pure torsion resonance with little bending oscillation at resonance. Figure 2 shows the torsional oscillation amplitude of a cantilever as a function of the excitation frequency in air as well as in water. For the fundamental torsional mode, this cantilever has a resonance at $\sim 200 \text{ kHz}$ ($\sim 140 \text{ kHz}$) with a Q factor of ~ 550 (~ 70) in air (in water). For the fundamental flexural bending mode, a resonance at $\sim 10 \text{ kHz}$ with a Q factor of ~ 25 is measured in air. However, we cannot detect the resonance of the fundamental bending mode in water (estimated to be $\sim 3 \text{ kHz}$ using Sader's method [25]), probably due to its very low Q factor resulting from strong energy dissipation for the flexural vibration of the long cantilever. Amazingly, both the resonant frequency and the Q factor of the torsion mode are about two orders of magnitude higher than those of the bending mode in water.

Figure 3 show the measured frequency shift of the torsion resonance versus the sample displacement for three different occasions. In all of these cases, a sharp jump in the resonant frequency shift occurs beyond a certain threshold point (indicated with a red dashed line in each case) during the tip approach and no frequency shift is detected before that. This is probably related to the sharply increasing in-plane stiffness upon contact with the sample surface, which provides an additional restoring force for the torsional oscillation. The normal force measured simultaneously in the above three cases shows that the sharp increase in the resonant frequency can occur in either the attractive or the repulsive regime. This reflects that the frequency shift of the TR mode is independent

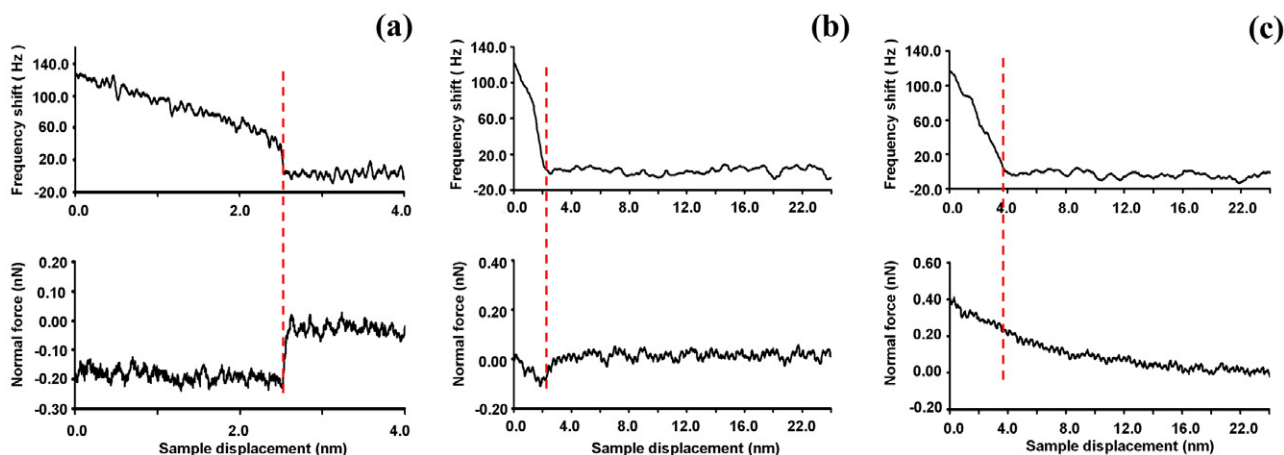


Figure 3. Frequency shift of the torsion resonance versus the sample displacement measured on three different occasions. Notice that the resonant frequency increases monotonically with decreasing sample displacement. The normal forces are also measured simultaneously and shown below.

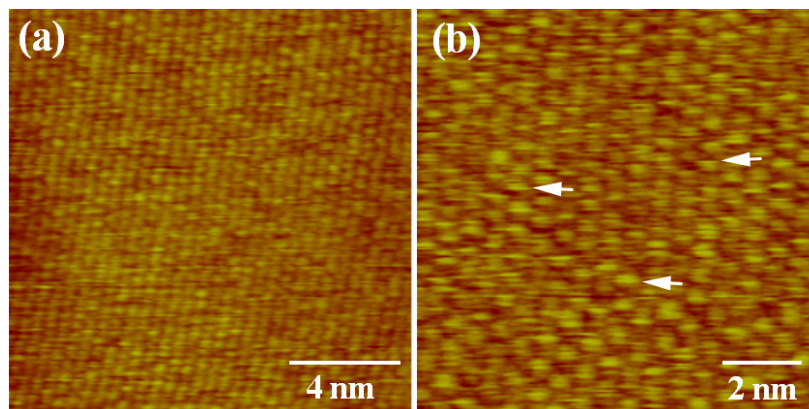


Figure 4. (a) and (b) Unfiltered AFM images of a mica surface in pure water taken with the FM-TR mode at $\Delta f = +18$ Hz. The torsional resonance frequency of the cantilever is ~ 90.28 kHz and the Q factor is ~ 51 . The free lateral oscillation amplitude is 0.9 nm. The pixel size of both images is 256×256 . The scan rate is 60 Hz, which is the highest scan rate of our AFM controller. We note that the lattice becomes more distorted as the scan rate is decreased, probably due to the thermal drift between the tip and the sample. Notice that many atoms do not appear as full circles. They often appear bright only for several scan lines (some examples are indicated with arrows). The fast scan direction is from left to right of the image.

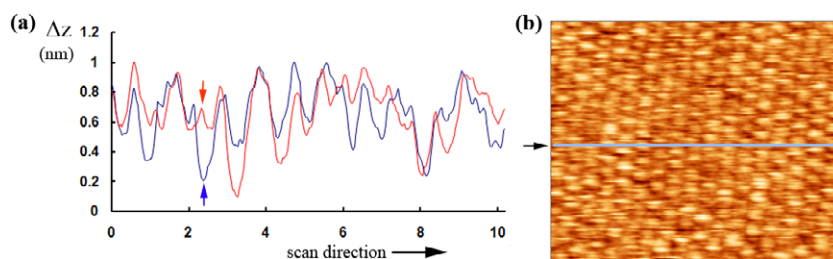


Figure 5. (a) Line profiles for two consecutive scan lines along the blue line indicated in the AFM image shown in (b). The red (blue) line profile is associated with the upper (lower) scan line. The two line profiles have almost identical protrusion positions. A red arrow indicates a protrusion in the upper profile, but this protrusion disappears in the next profile as indicated by the blue arrow. This seems to indicate that the adsorbed atom (or ion) disappears suddenly during the scanning. The AFM image in (b) is just the upper section shown in figure 4(b).

of the long-range normal forces. Therefore, we can view the threshold position as the contact point. It is also easy to maintain a stable feedback operation of the AFM at the initial jump of the resonant frequency. Our set point for feedback control is usually at a frequency shift less than 20 Hz or 0.1–1 nm from the contact point, so the normal forces are estimated to be a few pN to 80 pN.

3.2. AFM imaging on mica surfaces in water

By operating the FM-TR mode in the soft-contact regime as described above, we can achieve atomic resolution on a mica surface in water. As shown in figures 4(a) and (b), the atomic lattice on a mica surface can be clearly observed. The approach curve shown in figure 3(a) is measured on such a kind of surface. It indicates that the tip is operated stably in the attractive regime. In figure 4(b), atomic-scale bright spots can be clearly discerned. Notice that these spots often appear bright for only a few scan lines, suggesting some dynamics involved on the mica surface. Also, some spots appear brighter than others, suggesting different ion species are involved. Similar images of different bright spots and their dynamics are obtained several times using other AFM cantilevers of the same type. We suspect this is due to adsorption and desorption of individual positive ions on the mica surface. The

height profiles shown in figure 5 clearly indicate the sudden disappearing of a protrusion. The mica sample we use here is not pure muscovite mica; we suspect that there are positive ions different from K^+ ions, such as Na^+ , dissolved into the water after the surface cleavage. These ions may be adsorbed onto the surface momentarily.

Amazingly, negligible lateral force is detected on the mica surface in our soft-contact FM-TR mode operation. The typical friction loop, obtained by recording the dc value of the cantilever twist during scanning forward and backward across the sample surface, can reveal the amount of lateral force exerted by the scanning tip. In the friction loop shown in figure 6(a), a large hysteresis loop with a strong lateral force of ~ 1.8 nN is detected with the contact mode. By switching to the FM-TR mode with the same cantilever (figure 6(b)), the hysteresis loop disappears, indicating a very small lateral force is produced. Due to the capability to achieve a high spatial resolution and low normal and lateral forces on the sample surface, this soft-contact AFM mode would be ideal for imaging soft biological samples in liquid.

3.3. AFM imaging of DNA on mica surfaces in water

Figure 7(a) shows an AFM image of a DNA molecule on a mica surface taken with the FM-TR mode in water.

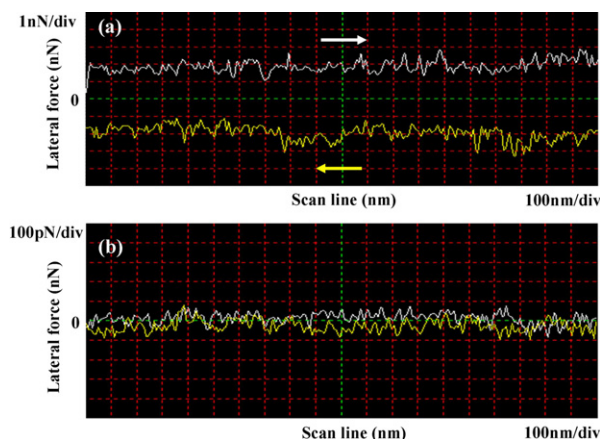


Figure 6. Measured lateral forces on a mica surface in pure water taken with the contact mode (a) and with the FM-TR mode (b). Each scan loop takes 1 s. The normal force is set at ~ 0.9 nN for the contact mode, which is the typical set point for stable contact mode imaging. Due to the thermal drifts of the system, operation at lower set forces would result in occasional instability in imaging. For the FM-TR mode, $\Delta f = +20$ Hz and the free lateral oscillation amplitude is 0.85 nm. The estimated lateral force applied on the mica surface is less than 50 pN. The flexural spring constant of the cantilever is measured to be 0.04 N m^{-1} and the torsion spring constant is estimated to be 7.1 N m^{-1} .

Figures 3(b) and (c) are typical approach curves taken on the mica surface and on the DNA molecule, respectively, in this kind of environment. It indicates that the scanning tip is operated in the attractive regime on the mica surface and in the repulsive regime on the DNA. We note that clear and stable images of DNA molecules like this can be acquired continuously with no change in the relative position of the DNA molecules. The resolution of the image is comparable to one obtained by a sharp carbon nanotube AFM tip [26]. However, every time when we switch to the contact mode, the images of the DNA become fuzzy, and damage and displacement of some parts of the molecules often occur during imaging even if the set force is minimized.

Typical AFM images are two-dimensional mapping of the z piezo-displacement (Δz), which is also the case for the image shown in figure 7(a). However, the bending of the cantilever caused by the normal forces may vary from site to site, and thus the flexural deflection has to be taken into account for the height measured from the Δz image. Figure 7(b) shows the flexural deflection image recorded simultaneously with the image shown in figure 7(a). It indicates a larger flexural deflection toward the repulsive regime on the DNA molecule than on the mica surface. A corrected topographic image can be obtained by combining the two images in figures 7(a) and (b). This corrected image (not shown) appears very similar to that shown in figure 7(a) but with a stronger contrast for the DNA molecule. A corrected height profile and the corresponding line profiles in figures 7(a) and (b) along the white dashed line in figure 7(a) is depicted in figure 7(c). The measured height, 2.25 nm, is very close to the diameter of duplex DNA determined by x-ray diffraction (~ 2.0 nm) [27], indicating that the AFM tip applies a very small loading force on the DNA molecule. We note that the flexural deflection

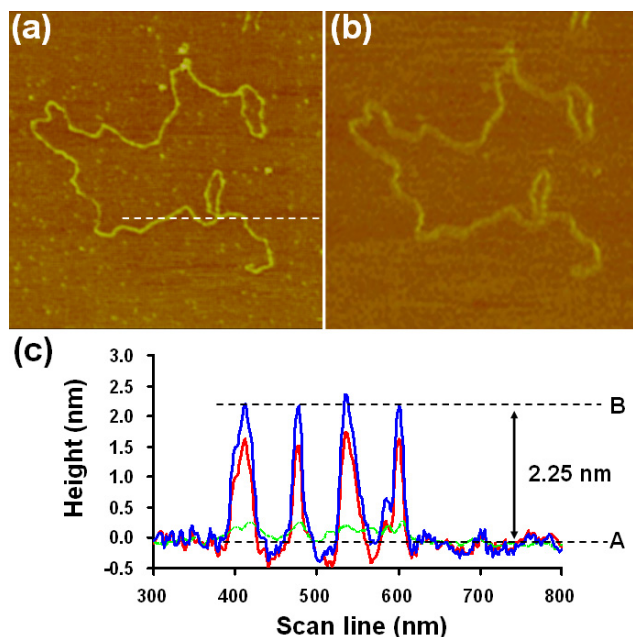


Figure 7. Measurements of duplex DNA on a mica surface in water. (a) AFM image taken with the FM-TR mode at $\Delta f = +16$ Hz. The free oscillation amplitude is 0.5 nm. Scan area: $800 \text{ nm} \times 800 \text{ nm}$. The torsional resonant frequency of the cantilever is ~ 103.95 kHz and the Q factor is ~ 52 . (b) Flexural deflection image of the cantilever recorded simultaneously with (a). (c) Line profiles along the dotted line in (a). Red, green and blue traces correspond to the profiles obtain in (a), (b) and the corrected height, respectively. Line A indicates the average height of the mica substrate and line B indicates an average height of the DNA. From the full width at half-maximum value of the measured width of the DNA, we can estimate that the size of the tip apex is about 12 nm. We note that there is no need to do such a height correction for the typical contact mode because the topographic images are taken at a constant flexural bending of the cantilever.

difference between DNA and mica seen in figure 7(b) is not as dramatic as that shown in figures 3(b) and (c). The absolute value for this difference varies with the tip apex condition and the ion concentration of the solution. It is very difficult to maintain a well-controlled ion concentration for our set-up shown in figure 1. Moreover, the concentration varies with time due to water evaporation. However, the flexural deflection is always toward the repulsive regime on DNA than on mica.

4. Discussion

4.1. Advantages of TR modes over flexural modes in AFM imaging

As clearly shown in figure 3, the resonance frequency of torsion resonance is a monotonic function of the sample displacement, but the normal force is often not. In fact, the approach curves for static or dynamic flexural modes are usually not monotonic and stable feedback is only possible on a branch of the approach curves where it is monotonic. Moreover, the torsion resonance frequency exhibits a sharp increase upon contact, which is very favorable for high-resolution imaging. This is similar to the behavior of the tunneling current in scanning tunneling microscopy (STM),

which exhibits a monotonic and sharply increasing function during tip approach. The tip used in STM usually has a radius much larger than that of most AFM tips. It is generally believed that a single-atom protrusion, even on top of a relatively large tip, would dominate the contribution of the total tunneling current, so STM can easily achieve atomic resolution on atomically flat surfaces. However, true atomic resolution on flat surfaces is very difficult for flexural AFM modes and very sharp tips are essential for high-resolution imaging. This is because the flexural AFM modes involve long-range interactions, which can seriously degrade the spatial resolution of AFM. In our FM-TR mode, the Au-coated tips have a nominal radius of 50 nm, equivalent in size to typical STM tips but much larger than most AFM tips used for high-resolution imaging. The major reason why we can resolve individual atomic features with such large tips is because the torsional oscillation is not sensitive to the long-range normal interactions.

As shown in figure 4, the AFM images are acquired in the attractive regime. Operation in this regime is very difficult for the contact mode. For our FM-TR modes, the loading force of the tip apex can be very small because the restoring force of the cantilever can balance the long-ranged attractive tip-sample interactions. It was reported that true atomic resolution could be achieved in water when the AFM probe was operated in the attractive regime [2]. However, the atomic images were acquired with no feedback control, which is acceptable for atomically flat surfaces but not suitable for surfaces with a certain degree of corrugation. For the AFM imaging of DNA on mica with the FM-TR mode (please refer to figures 3(b) and (c)), the AFM probe might be operated in the attractive regime on the mica surface but in the repulsive regime on DNA. Stable imaging with soft contact in these two different regimes is also very difficult for the flexural modes.

Müller *et al* have demonstrated that high-resolution images of biological samples can be taken in liquid with the contact mode AFM [3]. They carefully adjust ion concentrations in a buffer before AFM imaging, so that the long-range normal forces resulting from electrostatic interactions and van der Waals forces can be balanced [3], resulting in loading forces smaller than 100 pN. However, this method requires skillful manipulation of the electrolyte and it may make the solution different from physiological conditions. An advantage for the soft-contact FM-TR mode is that there is no need to balance the long-range normal forces and it allows investigators to probe biological molecules under a suitable physiological/pathological situation. In addition, this method is also not as sensitive to thermal drifts as the contact mode, which requires manual adjustment of the set force constantly during image acquisition [3].

For the TR mode, there is some concern about the lateral resolution because the tip is oscillating laterally. Resolving individual atomic features on mica surfaces indicates good lateral resolution with our FM-TR mode. For the TR mode, one does not need to worry about a low signal-to-noise ratio for a small oscillation amplitude as in the flexural resonance. The laser beam-deflection method used in typical AFMs is sensitive to the angular changes of the cantilever, rather than

the absolute oscillation distance, since a typical AFM tip height is $\sim 10 \mu\text{m}$, which is much shorter than the length of the cantilever (typically 100–400 μm). Therefore, the lateral oscillation amplitude of 1 nm in torsional oscillation yields an angular change equivalent to that of the vertical oscillation amplitude of 10–40 nm in the flexural bending. Therefore, good signal-to-noise ratio in the lateral oscillation amplitude of $< 1 \text{ nm}$ can be achieved easily with the optical detection system in most of the commercial AFMs. Fukuma *et al* achieved high force sensitivity in liquid by operating at the vertical oscillation amplitude of 0.1–0.3 nm [14, 16], which is a feat that cannot be achieved with current commercial AFMs. Fukuma *et al* have optimized their optical detection system to achieve a noise level one to two orders of magnitude lower than that of commercial AFM systems [28]. In our experimental set-up, we need to add frequency-modulation electronics through a signal access module of the commercial SPM controller. The long cables and the module add more noise to our detection system. Nevertheless, we still can get atomic features on mica surfaces with relatively large tips. This reflects the elegance and great potential of the FM-TR mode in liquid.

As we have demonstrated in this work, the Q factor and the resonant frequency of the first torsion resonance in water is significantly higher than those of the fundamental flexural resonance, and thus the TR mode can achieve a higher force sensitivity. Also, the much higher resonant frequency for the TR mode is beneficial for high-speed scanning. To achieve a resonant frequency significantly higher than 1 MHz for the first flexural resonance, one has to use a much smaller cantilever than those used in current tapping mode cantilevers. This makes the focusing of the detection laser spot inside the cantilever very challenging. With the TR mode, the requirement for the small size of the cantilever is not as stringent.

In addition, the combination of the FM-TR mode with compliant cantilevers can allow the measurement of the normal forces simultaneously. It is not only good for the force curve measurements, but also very promising for future development of charge or potential mapping in liquid because the major contribution for the normal forces in liquid is the electrostatic force. In fact, the image contrast shown in figure 7(b) mainly results from the difference in the electrostatic forces (please also refer to figures 3(b) and (c)). Current AFM methods to map surface charges in liquid are based on the flexural modes [29–31]. They are tedious and neither the force sensitivity nor the spatial resolution is good.

4.2. Other discussions related to TR modes

Our lateral resolution on DNA is measured to be about 12 nm, which is mainly limited by the relatively large tip size. The reason we cannot use AFM probes with sharper tips is because very few types of AFM cantilevers exhibit clear torsion resonance in water. Current AFM cantilevers are mainly designed for flexural modes and are not optimized for torsional oscillation because the TR modes are not commonly adopted. This may require further experimental and theoretical studies to understand the appropriate probe geometry for pure

torsion resonance. We anticipate better TR cantilevers with sharp tips can further improve the force sensitivity and spatial resolution of the TR modes.

From the approach curves shown in figures 3(b) and (c), it can be seen that the slope of the frequency shift on mica and on DNA are different. The slope may reflect the mechanical properties of the sample surfaces. It would be desirable to have theoretical studies on the cantilever dynamics and the tip motion for the torsion resonance in liquid, especially during the initial contact with a soft material. This would help the characterization of the sample surface.

The operation of the TR mode in water with the amplitude as the feedback signal was recently reported by Mullin and Hobbs [32]. We have also tried this AM-TR mode. The image quality is close to that taken with the FM-TR mode even though not as good. We do not use the AM-TR mode as often as the FM-TR mode because sometimes the amplitude versus the sample displacement is not monotonic, which makes the stable feedback operation more difficult and the image quality not as consistent as in the FM-TR mode.

Current UHV-AFMs can achieve atomic resolution on flat and hard surfaces with dangling bonds (reactive surfaces), such as silicon surfaces [5–11]. These AFMs usually use the strong attractive chemical forces between the tip atom and the surface atom to resolve surface atomic structures. However, they have great difficulty in obtaining atomic resolution in imaging non-reactive surfaces. Very recently, Gross *et al* reported atomic resolution of pentacene molecules at 5 K in vacuum by terminating the tip with a CO molecule [12]. They concluded that Pauli repulsion is the source of atomic resolution. The soft-contact FM-TR mode may also be useful for imaging surface atomic structures in vacuum, if the tip can be properly passivated such that the contribution from chemical interactions is small. It is likely that the use of Pauli repulsion can yield atomic resolution in most situations.

5. Conclusions

We have presented a soft-contact FM-TR mode which can achieve high-resolution imaging in liquid with small normal and lateral forces. Atomic features on mica surfaces can be resolved in water even with a relatively large tip. This method may allow development of high-sensitivity, high-resolution and high-speed AFMs in liquid, which is especially important for the study of biological processes in physiological conditions. Therefore, it is urgent to understand the cantilever's dynamics and the tip motion for the torsion resonance in liquid theoretically. This would help optimizing the imaging conditions and characterization of many properties of soft materials in liquid.

Acknowledgments

This research is supported by the National Science Council of ROC (contract no. NSC96-2628-M-001-010-MY39) and Academia Sinica.

References

- [1] Binnig G, Quate C F and Gerber C 1986 *Phys. Rev. Lett.* **56** 930
- [2] Ohnesirge F and Binnig G 1993 *Science* **260** 1451
- [3] Müller D J, Fotiadis D, Scheuring S, Müller S A and Engel A 1999 *Biophys. J.* **76** 1101
- [4] Albrecht T R, Grütter P, Horne D and Rugar D 1991 *J. Appl. Phys.* **69** 668
- [5] Giessible F J 2003 *Rev. Mod. Phys.* **75** 949
- [6] Giessible F J 1995 *Science* **267** 68
- [7] Sugawara Y, Ohta M, Ueyama H and Morita S 1995 *Science* **270** 1646
- [8] Lantz M A *et al* 2001 *Science* **291** 2580
- [9] Eguchi T and Hasegawa Y 2002 *Phys. Rev. Lett.* **89** 266105
- [10] Oyabu N *et al* 2005 *Nanotechnology* **16** S112
- [11] Sugimoto Y *et al* 2007 *Nature* **446** 64
- [12] Gross L, Mohn F, Moll N, Liljeroth P and Meyer G 2009 *Science* **325** 1110
- [13] Yang C-H, Hwang I-S, Chen Y F, Chang C S and Tsai D P 2007 *Nanotechnology* **18** 084009
- [14] Fukuma T, Kobayashi K, Matsushige K and Yamada H 2005 *Appl. Phys. Lett.* **87** 034101
- [15] Hoogenboom B W *et al* 2006 *Appl. Phys. Lett.* **88** 193109
- [16] Fukuma T and Jarvis S P 2006 *Rev. Sci. Instrum.* **77** 043701
- [17] Rief M, Oesterhelt F, Heymann B and Gaub H E 1997 *Science* **275** 1295
- [18] Oesterhelt F *et al* 2000 *Science* **288** 143
- [19] Su C, Huang L, Neilson P and Kelley V 2003 *Scanning Tunneling Microscopy/Spectroscopy and Related Techniques: 12th Int. Conf.* ed P M Koenraad and M Kemerink p 349
- [20] Huang L and Su C 2004 *Ultramicroscopy* **100** 277
- [21] Kasai T, Bhushan B, Huang L and Su C 2004 *Nanotechnology* **15** 731
- [22] Reinstädler M, Kasai T, Rabe U, Bhushan B and Arnold W 2005 *J. Phys. D: Appl. Phys.* **38** R269
- [23] Gneco E *et al* 2000 *Phys. Rev. Lett.* **84** 1172
- [24] Jeon S and Braiman Y 2004 *Appl. Phys. Lett.* **84** 10
- [25] Eysden C A V and Sader J E 2006 *J. Appl. Phys.* **100** 114916
- [26] Martinez J, Yuzvinsky T D, Fennimore A M, Zettl A, Garcia R and Bustamante C 2005 *Nanotechnology* **16** 2493
- [27] Saenger W 1984 *Principles of Nucleic Acid Structure* (Berlin: Springer)
- [28] Fukuma T, Kimura M, Kobayashi K, Matsushige K and Yamada H 2005 *Rev. Sci. Instrum.* **76** 053704
- [29] Heinz W F and Hoh J H 1999 *Biophys. J.* **76** 528
- [30] Noort S J T v, Willemsen O H, Werf K O v d, Grooth B G d and Greve J 1999 *Langmuir* **15** 7101
- [31] Yang Y, Mayer K M and Hafner J H 2007 *Biophys. J.* **92** 1966
- [32] Mullin N and Hobbs J 2008 *Appl. Phys. Lett.* **92** 053103